

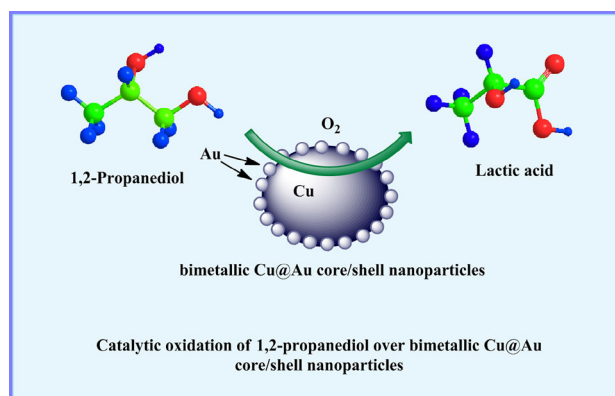
# Catalytic Oxidation of 1,2-Propanediol over Bimetallic Cu@Au Core/Shell Nanoparticles

Wuping Xue<sup>1</sup> · Hengbo Yin<sup>1</sup> · Zhipeng Lu<sup>1</sup> · Yonghai Feng<sup>1</sup> · Aili Wang<sup>1</sup> · Shuxin Liu<sup>2</sup> · Lingqin Shen<sup>1</sup> · Xingyuan Jia<sup>1</sup>

Received: 6 March 2016 / Accepted: 22 March 2016  
© Springer Science+Business Media New York 2016

**Abstract** Bimetallic Cu@Au core/shell nanoparticles were prepared by the wet chemical reduction method using Tween as the organic modifier. The Cu@Au nanoparticles exhibited higher catalytic activity for the oxidation of 1,2-propanediol under mild reaction conditions than the sole Au nanoparticles. The Cu@Au nanoparticles with the mole ratios of Au to Cu of 0.015:0.985 and 0.035:0.965 exhibited high catalytic activities for the catalytic oxidation of 1,2-propanediol to lactic acid. A power function type reaction kinetic model well fitted the experimental data over the Cu<sub>0.985</sub>Au<sub>0.015</sub> nanoparticle catalyst,  $r = -dn_0 / (dt \cdot W_{cat}) = kC_0^{0.49}P_0^{0.39}$ , and the reaction activation energy was 34.1 kJ mol<sup>-1</sup>.

## Graphical Abstract



**Keywords** 1,2-Propanediol oxidation · Bimetallic Cu@Au nanoparticles · Lactic acid · Reaction kinetics

## 1 Introduction

Lactic acid is an important commodity chemical and has abundant applications in the food, pharmaceutical, and cosmetic industries [1–7]. Lactic acid as one of the top 12 biobased platform molecules has been used as the raw material for the synthesis of a series of chemicals [8, 9].

Commercial lactic acid is conventionally produced via the carbohydrate fermentation process. This process has some disadvantages, such as large amount of water spending, low reaction rate, and high cost, due to its downstream separation and purification from the fermentation broth [5, 7, 10]. Furthermore, biological sludge is produced in the carbohydrate fermentation process [11, 12]. To overcome these disadvantages, environmental friendly chemical routes have attracted the interest of researchers.

**Electronic supplementary material** The online version of this article (doi:10.1007/s10562-016-1736-3) contains supplementary material, which is available to authorized users.

✉ Hengbo Yin  
yin@ujs.edu.cn

<sup>1</sup> Faculty of Chemistry and Chemical Engineering, Jiangsu University, Zhenjiang 212013, People's Republic of China

<sup>2</sup> School of Chemistry and Chemical Engineering, Mianyang Normal University, Mianyang 621000, People's Republic of China

Lactic acid can be synthesized via the reaction of acetaldehyde with HCN followed by the hydrolysis with sulfuric acid. In the synthesis process, both toxic HCN and corrosive sulfuric acid are used as the raw material and catalyst, respectively, which could cause seriously environmental problems [13, 14]. Accompanied with the scaling-up production of dimethyl carbonate by the transesterification method [15], 1,2-propanediol market faces oversupply, especially in China [16, 17]. However, the oversupplied 1,2-propanediol can be used as an alternative raw material for synthesizing lactic acid via catalytic oxidation route.

Lactic acid can be synthesized by the catalytic oxidation of 1,2-propanediol over monometallic and bimetallic Au, Pd, Ag, and Pt catalysts in an alkaline medium [11, 13, 18–23]. Tsujino et al. [18] and Pinxt et al. [19] reported the oxidation of 1,2-propanediol over Pd/C and Pt/graphite modified with Pd, Bi, Te, and/or Sn catalysts, in which, the main product was pyruvic acid rather than lactic acid. Although the results for the catalytic oxidation of 1,2-propanediol to lactic acid were unsatisfactory, these pioneer studies revealed that 1,2-propanediol can be catalytically converted to lactic acid. Prati et al. [13] reported that 1 %Au/C catalyst exhibited high catalytic activity for the oxidation of 1,2-propanediol with O<sub>2</sub> to lactic acid with the lactic acid yield of 100 % at the 1,2-propanediol conversion of 78 % at 90 °C for 1 h in an alkaline medium. Xu et al. [20] investigated the effect of support types on the conversion of 1,2-propanediol to lactic acid over supported Au catalysts. It was found that Au/MgO catalyst exhibited higher catalytic activity than the Au/graphite and Au/TiO<sub>2</sub> catalysts [21, 24]. When the reaction was carried out over Au/MgO catalyst under 0.3 MPa of O<sub>2</sub> at 60 °C for 6 h, the lactic acid selectivity was 89.3 % at the 1,2-propanediol conversion of 94.4 %. Our previous work revealed that over Au<sub>0.75</sub>Pd<sub>0.25</sub>/Mg(OH)<sub>2</sub> and Au<sub>0.75</sub>Pd<sub>0.25</sub>/HAP catalysts, the 1,2-propanediol conversion and lactic acid selectivity were more than 96 and 88 %, respectively [11, 22]. The previous work revealed that Au-containing noble bimetallic catalysts exhibited high catalytic activities for the oxidation of 1,2-propanediol to lactic acid. However, the high cost of these noble bimetallic catalysts may be a drawback for their practical application. Non-noble/noble bimetallic catalysts for the catalytic oxidation of 1,2-propanediol is worthy of investigation in the view point of lowering catalyst cost. To the best of our knowledge, the catalytic oxidation of 1,2-propanediol over non-noble/noble bimetallic catalysts has not been reported until now.

In our present work, the bimetallic Cu@Au core/shell nanostructures with Au nanoparticles epitaxially grown on the surfaces of Cu nanoparticles were prepared by the wet chemical reduction method in the presence of Tween as the organic modifier. The as-prepared Cu@Au core/shell

nanoparticles were used to catalyze the oxidation of 1,2-propanediol with O<sub>2</sub> to lactic acid in an alkaline aqueous solution under mild reaction conditions. The effect of the composition and particle size of Cu@Au nanoparticles on the catalytic oxidation of 1,2-propanediol to lactic acid was investigated. A power function-type reaction kinetic model was simulated to evaluate the reaction kinetics of 1,2-propanediol oxidation over the Cu@Au nanoparticle catalysts.

## 2 Experimental

### 2.1 Materials

Copper nitrate (Cu(NO<sub>3</sub>)<sub>2</sub>·3H<sub>2</sub>O), chloroauric acid (HAuCl<sub>4</sub>·3H<sub>2</sub>O), Tween-80 (Tween), hydrazine hydrate (N<sub>2</sub>H<sub>4</sub>·H<sub>2</sub>O), ethanol, sodium hydroxide (NaOH), 1,2-propanediol, lactic acid, formic acid, and acetic acid were of reagent grade and were purchased from Sinopharm Chemical Reagent Co., Ltd. China. Methanol was of chromatographic grade and was purchased from Sinopharm Chemical Reagent Co., Ltd. China. All the chemicals were used as received without further purification.

### 2.2 Preparation of Cu<sub>x</sub>Au<sub>y</sub> Nanoparticles

Cu<sub>x</sub>Au<sub>y</sub> nanoparticles (x and y, the mole ratios of Cu and Au in the sample) were prepared by the wet chemical reduction method with the use of hydrazine hydrate as the reductant and Tween-80 as the organic modifier. Typically, copper nitrate trihydrate (3.78 g) and Tween-80 (0.38 g) were dissolved in an anhydrous ethanol (120 mL) by ultrasonic treatment for 30 min. After the mixture was heated at 60 °C for 30 min, an ethanol solution of NaOH (1.5 M, 50 mL) was added dropwise to adjust the pH value of the reaction solution to 8–9. Then, a hydrazine hydrate ethanol solution (16.0 in 160 mL anhydrous ethanol) was added dropwise to the mixture at 60 °C for 2 h. After reduction, the color of the reaction solution changed to black, indicating that Cu<sup>2+</sup> was reduced to metallic Cu<sup>0</sup>. The as-prepared Cu nanoparticles were cooled to 30 °C and an ethanol solution of chloroauric acid (20 mL) was added dropwise to it at 30 °C for 1 h under mild stirring. The resultant Cu<sub>x</sub>Au<sub>y</sub> nanoparticles were centrifugated, washed with anhydrous ethanol, and dried at 60 °C in a vacuum oven overnight before they were characterized and used as catalysts for the oxidation of 1,2-propanediol.

For comparison, sole Cu nanoparticles were prepared according to the above-mentioned procedures. Cu<sub>0.985</sub>Au<sub>0.015</sub> nanoparticles were also prepared without the use of Tween-80 as the organic modifier, which were denoted as Cu<sub>0.985</sub>Au<sub>0.015</sub>-controlled. Sole Au nanoparticles were

prepared by using water as the solvent in the presence of Tween-80 as the organic modifier and the Au nanoparticles in the aqueous suspension were used as the catalyst without drying treatment.

### 2.3 Characterization

The X-ray powder diffraction (XRD) was used to examine the as-prepared nanoparticle samples. The XRD spectra of the samples were recorded on a diffractometer (D8 super speed Bruke-AEX Company, Germany) using Cu K $\alpha$  radiation ( $\lambda = 1.54056 \text{ \AA}$ ) with a Ni filter, scanning from  $20^\circ$  to  $80^\circ$  ( $2\theta$ ). The crystallite sizes of metallic Cu and Au, (111) planes, were calculated by using the Scherrer's equation:  $D = K\lambda/(B\cos\theta)$ , where  $K$  was taken as 0.89 and  $B$  was the full width of the diffraction line at half of the maximum intensity. The crystallite sizes of metallic Cu (111) and Au (111) of the samples are listed in Table 1.

Transmission electron microscopy (TEM) and high resolution transmission electron microscopy (HRTEM) images of the nanoparticle samples were obtained on a microscope (JEM-2100) operated at an acceleration voltage of 200 kV. The TEM specimens were prepared by placing a drop of ethanol suspension of nanoparticle sample onto a copper grid coated with a layer of amorphous carbon. The data used for the calculation of the particle size distribution for each sample was measured from the TEM and HRTEM images. The average particle sizes of Cu and Au nanoparticles were calculated by a weighted-average method according to the individual particle sizes of the all counted particles.

X-ray photoelectron spectra (XPS) of the catalysts were recorded on an XSAM800 spectrometer (Kratos Company) using Al K $\alpha$  radiation (1486.6 eV). The binding energies were calculated with respect to C1 s peak of contaminated carbon at 284.6 eV.

### 2.4 Catalytic Test

The catalytic oxidation of 1,2-propanediol with O<sub>2</sub> was performed in a 1000 mL capacity stainless steel autoclave equipped with a magnetic stirrer. The autoclave was charged with appointed amounts of 1,2-propanediol, sodium hydroxide, water, and catalyst. Firstly, the autoclave was purged with N<sub>2</sub> for 10 min to replace the present air. After the given reaction temperature was reached at the stirring speed of 100 rpm (for heating evenly), pure O<sub>2</sub> was pressurized to the desired pressure and the oxidation of 1,2-propanediol started at the stirring speed of 600 rpm. After reacting for a given time period, the autoclave was cooled to ambient temperature and depressurized for product analysis.

Before product analysis, the reaction mixture was acidified with hydrochloric acid (12 M) to the pH value of ca. 3. The concentration of remaining 1,2-propanediol was analyzed on a gas-phase chromatograph equipped with a PEG-20 M packed capillary column (0.25 mm  $\times$  30 m) and a FID by the internal standard method with *n*-butanol as the internal standard. The products, such as formic acid, lactic acid, and acetic acid, were analyzed on a Varian HPLC system equipped with a reverse-phase column (Chromspher 5 C18, 4.6 mm  $\times$  250 mm) and a UV detector ( $\lambda = 210 \text{ nm}$ ) at 30 °C. The mobile phase was

**Table 1** Physicochemical properties of the nanoparticle samples

Catalysts	Raw materials (g)		Cu/Au atomic ratios <sup>a</sup>	Crystallite sizes of Cu and Au (nm) <sup>b</sup>		Particle sizes of Cu and Au (nm) <sup>c</sup>		Binding energies (eV)			
	Cu(NO <sub>3</sub> ) <sub>2</sub> ·3H <sub>2</sub> O	AuCl <sub>3</sub> ·HCl·4H <sub>2</sub> O		Cu (111)	Au (111)	Cu	Au	Cu2p <sub>1/2</sub>	Cu2p <sub>3/2</sub>	Au4f <sub>5/2</sub>	Au4f <sub>7/2</sub>
Cu	3.78	0	/	27.0	/	60.5	/	952.6	932.6	/	/
Cu <sub>0.995</sub> Au <sub>0.005</sub>	3.78	0.03	0.995:0.028	25.3	3.9	61.1	4.9	952.6	932.5	87.50	83.90
Cu <sub>0.985</sub> Au <sub>0.015</sub>	3.78	0.10	0.985:0.033	25.0	4.1	60.3	5.0	952.5	932.4	87.55	83.95
Cu <sub>0.965</sub> Au <sub>0.035</sub>	3.78	0.23	0.965:0.039	24.3	4.2	60.8	5.3	952.4	932.3	87.65	84.05
Cu <sub>0.95</sub> Au <sub>0.05</sub>	3.78	0.34	0.95:0.053	24.4	4.0	59.9	5.2	951.9	932.0	87.70	84.10
Au	0	0.34	/	/	4.9	/	5.6	/	/	87.70	84.10
Cu <sub>0.985</sub> Au <sub>0.015</sub> -controlled	3.78	0.10	/	34.2	6.1	107	6.7	/	/	/	/

<sup>a</sup> The atomic ratios of Cu to Au were determined by XPS

<sup>b</sup> The crystallite sizes were calculated by Scherrer's equation

<sup>c</sup> The particle sizes were measured from TEM images

composed of  $\text{H}_3\text{PO}_4/\text{NaH}_2\text{PO}_4$  (0.1 M  $\text{NaH}_2\text{PO}_4$  acidified by  $\text{H}_3\text{PO}_4$  to  $\text{pH} = 2.3$ ) buffer aqueous solution and methanol of chromatographic grade (V:V = 9:1) with a flow rate of  $0.8 \text{ mL min}^{-1}$ . The concentrations of products were analyzed by the external standard method. The product selectivities were calculated on carbon basis.

### 3 Results and Discussion

#### 3.1 XRD Analysis

The XRD patterns of the samples prepared under different conditions are shown in Fig. 1. When pure Cu sample was prepared by using Tween as the modifier, three XRD diffraction peaks appearing at  $2\theta = 43.3^\circ$ ,  $50.4^\circ$ , and  $74.1^\circ$  were indexed as the (111), (200), and (220) planes of the face centered-cubic (fcc) copper (JCPDS 04-0836), respectively. There were no diffraction peaks of copper oxides or copper hydroxides detected by the XRD analysis, indicating that the as-prepared Cu sample was phase-pure metallic  $\text{Cu}^0$ . The XRD peaks of copper component for the  $\text{Cu}_{0.995}\text{Au}_{0.005}$ ,  $\text{Cu}_{0.985}\text{Au}_{0.015}$ ,  $\text{Cu}_{0.965}\text{Au}_{0.035}$ , and  $\text{Cu}_{0.95}\text{Au}_{0.05}$  samples appeared at  $2\theta = 43.5^\circ$ ,  $50.5^\circ$ , and  $74.3^\circ$ , respectively, which were ca.  $0.2^\circ$  higher than those of pure Cu sample. The XRD peaks of the pure Au sample appearing at  $2\theta = 38.2^\circ$ ,  $44.4^\circ$ ,  $64.6^\circ$ , and  $77.5^\circ$  were ascribed to those of the face centered-cubic (fcc) gold (JCPDS 46-1043). The XRD characteristic peaks of

metallic Au in the  $\text{Cu}_{0.995}\text{Au}_{0.005}$ ,  $\text{Cu}_{0.985}\text{Au}_{0.015}$ ,  $\text{Cu}_{0.965}\text{Au}_{0.035}$ , and  $\text{Cu}_{0.95}\text{Au}_{0.05}$  samples appeared at  $2\theta = 38.1^\circ$ , which could be indexed as the (111) plane of metallic Au. These peaks were ca.  $0.1^\circ$  lower than that of the pure Au sample. As compared to the XRD peaks of the pure Cu and Au samples, the XRD peak shifts of Cu and Au in the bimetallic  $\text{Cu}_x\text{Au}_y$  samples indicated that there probably existed an alloy trend between Cu and Au components.

The Cu (111) crystallite sizes of the pure Cu and bimetallic  $\text{Cu}_x\text{Au}_y$  samples were estimated by Scherrer's equation (Table 1). When Tween-80 was used as the organic modifier, the Cu (111) crystallite sizes (24.3–27.0 nm) of the pure Cu,  $\text{Cu}_{0.995}\text{Au}_{0.005}$ ,  $\text{Cu}_{0.985}\text{Au}_{0.015}$ ,  $\text{Cu}_{0.965}\text{Au}_{0.035}$ , and  $\text{Cu}_{0.95}\text{Au}_{0.05}$  samples were close to each other, which was due to the fact that Cu nanoparticles were first prepared before coating Au nanoparticles. The Au (111) crystallite sizes of the  $\text{Cu}_{0.995}\text{Au}_{0.005}$ ,  $\text{Cu}_{0.985}\text{Au}_{0.015}$ ,  $\text{Cu}_{0.965}\text{Au}_{0.035}$ , and  $\text{Cu}_{0.95}\text{Au}_{0.05}$  samples were ca. 4 nm, smaller than that of pure Au sample (4.9 nm). The results revealed that the interaction between the Au and Cu components in  $\text{Cu}_x\text{Au}_y$  samples favored the formation of small-sized Au nanoparticles. The Cu (111) and Au (111) crystallite sizes (34.2 and 6.1 nm) in the  $\text{Cu}_{0.985}\text{Au}_{0.015}$ -controlled sample prepared without organic modifier were larger than those of  $\text{Cu}_{0.985}\text{Au}_{0.015}$  sample, indicating that the presence of Tween-80 favored the formation of small-sized Au and Cu nanoparticles.

#### 3.2 TEM Analysis

The TEM and HRTEM images of the samples are shown in Fig. 2. The TEM images show that the monometallic Cu nanoparticles had the particle sizes ranging from 28 to 133 nm and the average particle size of 60.5 nm (Fig. 2a). The monometallic Au nanoparticles had the particle sizes ranging from 2.4 to 8.8 nm and the average diameter of 5.6 nm (Fig. 2f). The HRTEM image (inset of Fig. 2f) shows that the lattice fringes of Au nanoparticle were examined to be ca. 0.203 and 0.235 nm, close to the (111) and (200) lattice spacing of fcc metallic gold.

The TEM images of the bimetallic  $\text{Cu}_x\text{Au}_y$  samples prepared in the presence of Tween show that the Cu nanoparticles had similar average particle sizes of ca. 60 nm (Fig. 2b–e). The average particle sizes of the Au nanoparticles ranged from 4.9 to 5.3 nm. The HRTEM image of  $\text{Cu}_{0.995}\text{Au}_{0.005}$  sample (inset of Fig. 2b) shows that the Au nanoparticles were well anchored on the surfaces of Cu nanoparticles. The amount of the Au nanoparticles on the surfaces of Cu nanoparticles increased with increasing the Au content. The bimetallic nanoparticles had the Cu@Au core-shell structure.

When the  $\text{Cu}_{0.985}\text{Au}_{0.015}$ -controlled sample was prepared without using Tween as the organic modifier, the

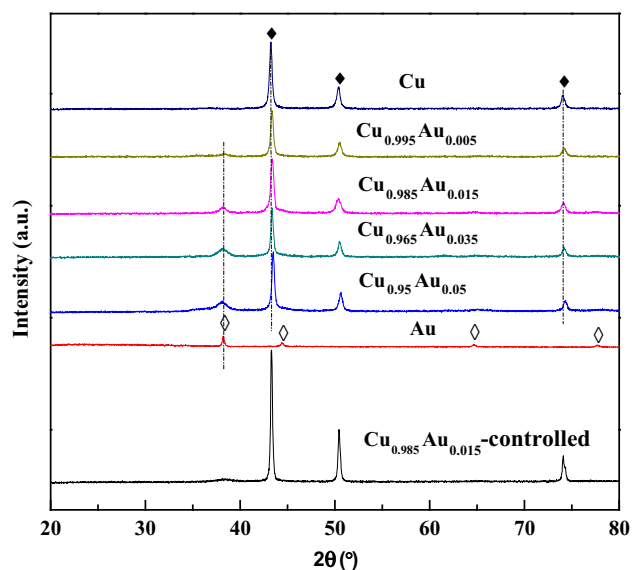
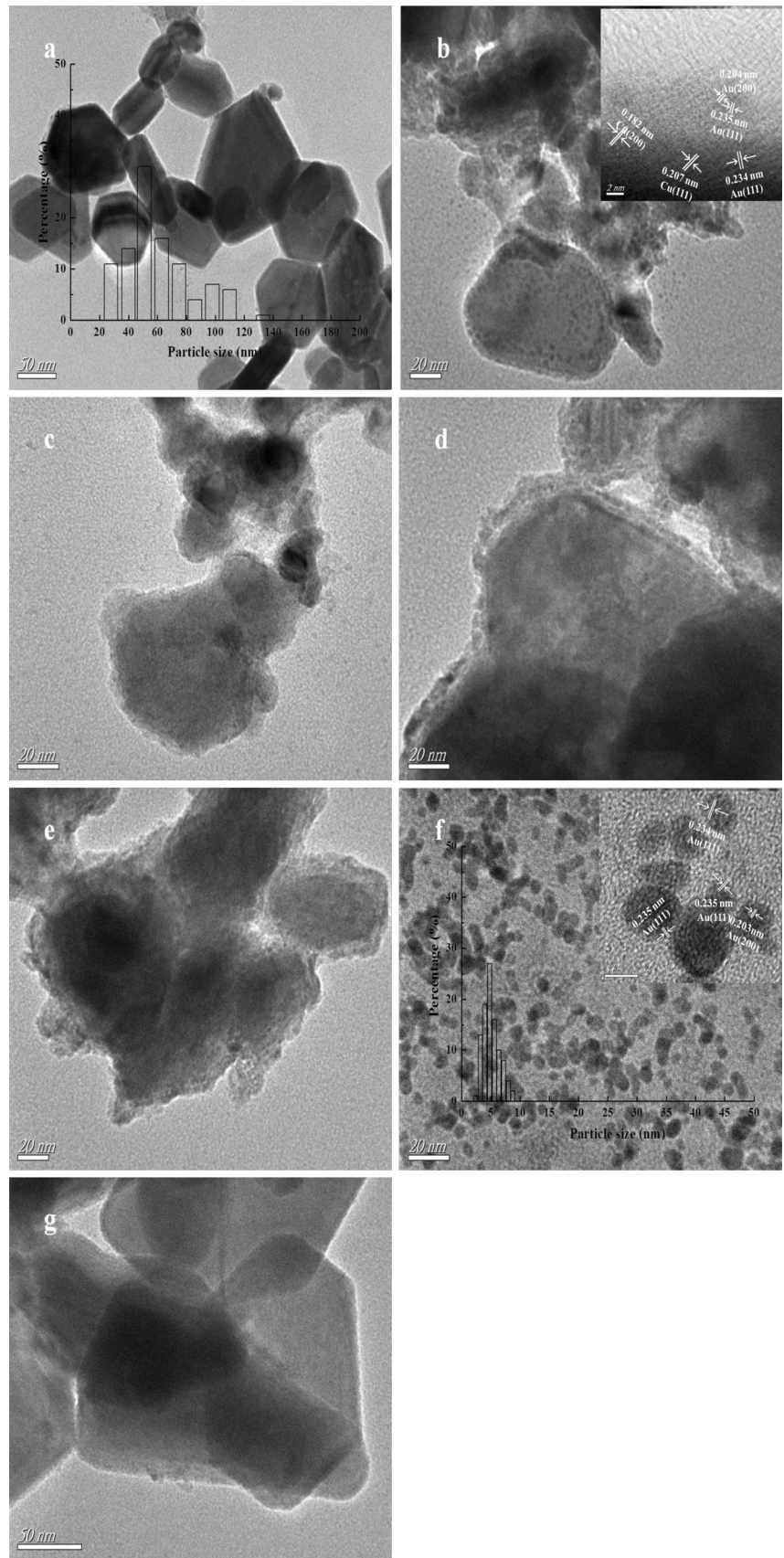


**Fig. 1** XRD patterns of Cu, Au,  $\text{Cu}_{0.95}\text{Au}_{0.05}$ ,  $\text{Cu}_{0.965}\text{Au}_{0.035}$ ,  $\text{Cu}_{0.985}\text{Au}_{0.015}$ , and  $\text{Cu}_{0.995}\text{Au}_{0.005}$  samples prepared by using Tween-80 as the organic modifier and  $\text{Cu}_{0.985}\text{Au}_{0.015}$ -controlled sample prepared without the use of organic modifier. Black diamond, Cu; open diamond, Au

**Fig. 2** TEM images of **a** Cu, **b**  $\text{Cu}_{0.995}\text{Au}_{0.005}$ , **c**  $\text{Cu}_{0.985}\text{Au}_{0.015}$ , **d**  $\text{Cu}_{0.965}\text{Au}_{0.035}$ , **e**  $\text{Cu}_{0.95}\text{Au}_{0.05}$ , and **f** Au samples prepared with the use of Tween-80 as the organic modifier and **g**  $\text{Cu}_{0.985}\text{Au}_{0.015}$ -controlled sample prepared without the use of organic modifier, and HRTEM images of  $\text{Cu}_{0.995}\text{Au}_{0.005}$  (**b**) and Au (**f**) samples



metallic Cu and Au nanoparticles had the average particle sizes of ca. 107 and 6.7 nm, respectively (Fig. 2g). The results revealed that the presence of organic modifier favored the formation of small-sized Au and Cu nanoparticles in the bimetallic  $\text{Cu}_x\text{Au}_y$  samples, which was consistent with the result obtained by XRD analysis.

### 3.3 XPS Analysis

The XPS measurement was employed to determine the surface chemical states and compositions of the bimetallic  $\text{Cu}_x\text{Au}_y$  samples. The XPS spectra of Cu2p and Au4f are shown in Fig. 3a, b. The binding energies of Cu2p and Au4f and the atomic ratios of Cu to Au are listed in Table 1.

The binding energies of  $\text{Au}4f_{5/2}$  and  $\text{Au}4f_{7/2}$  for the pure Au and  $\text{Cu}_x\text{Au}_y$  samples were in the ranges of 87.5–87.7 and 83.9–84.1 eV, respectively, indicating that the Au nanoparticles were metallic gold [25]. The binding energies of  $\text{Cu}2p_{1/2}$  and  $\text{Cu}2p_{3/2}$  for the pure Cu and  $\text{Cu}_x\text{Au}_y$  samples were in the ranges of 951.9–952.6 and 932.0–932.6 eV, respectively. To ascertain the chemical states of the Cu nanoparticles present in the samples, the Wagner plots are drawn and shown in Fig. 3c. The kinetic energy (KE) of the Auger transition and the  $\text{Cu}2p_{3/2}$  binding energy of the photoemission were taken as Y and X axes, respectively. The data for Cu,  $\text{Cu}_2\text{O}$ , and CuO reference samples were taken from Ref. [26]. It was found that the copper specie present in the pure Cu and  $\text{Cu}_x\text{Au}_y$  samples was metallic  $\text{Cu}^0$  because the Auger parameters of the samples fell on the line of metallic copper.

The binding energies of  $\text{Cu}2p_{1/2}$  and  $\text{Cu}2p_{3/2}$  for the bimetallic  $\text{Cu}_x\text{Au}_y$  nanoparticle samples decreased with the decrease in Cu/Au atomic ratios. The binding energies of  $\text{Au}4f_{5/2}$  and  $\text{Au}4f_{7/2}$  in the bimetallic  $\text{Cu}_x\text{Au}_y$  nanoparticle samples were close to those of the pure Au nanoparticles. The binding energy shifts of Cu2p for the bimetallic  $\text{Cu}_x\text{Au}_y$  nanoparticles were probably due to the alloy trend between Cu and Au nanoparticles. Furthermore, the XPS analysis revealed that the atomic ratios of Cu to Au determined by XPS were smaller than those calculated according to their precursor compositions, revealing that Au nanoparticles anchored on the surfaces of metallic Cu nanoparticles.

### 3.4 Oxidation of 1,2-Propanediol Catalyzed by $\text{Cu}_x\text{Au}_y$ Nanoparticles

The catalytic activities of the  $\text{Cu}_x\text{Au}_y$  nanoparticles for the catalytic oxidation of 1,2-propanediol under 1.0 MPa of  $\text{O}_2$  at 100 °C for 4 h are listed in Table 2. Lactic acid, acetic acid, and formic acid were formed as the main products and no other product was detected. When the monometallic

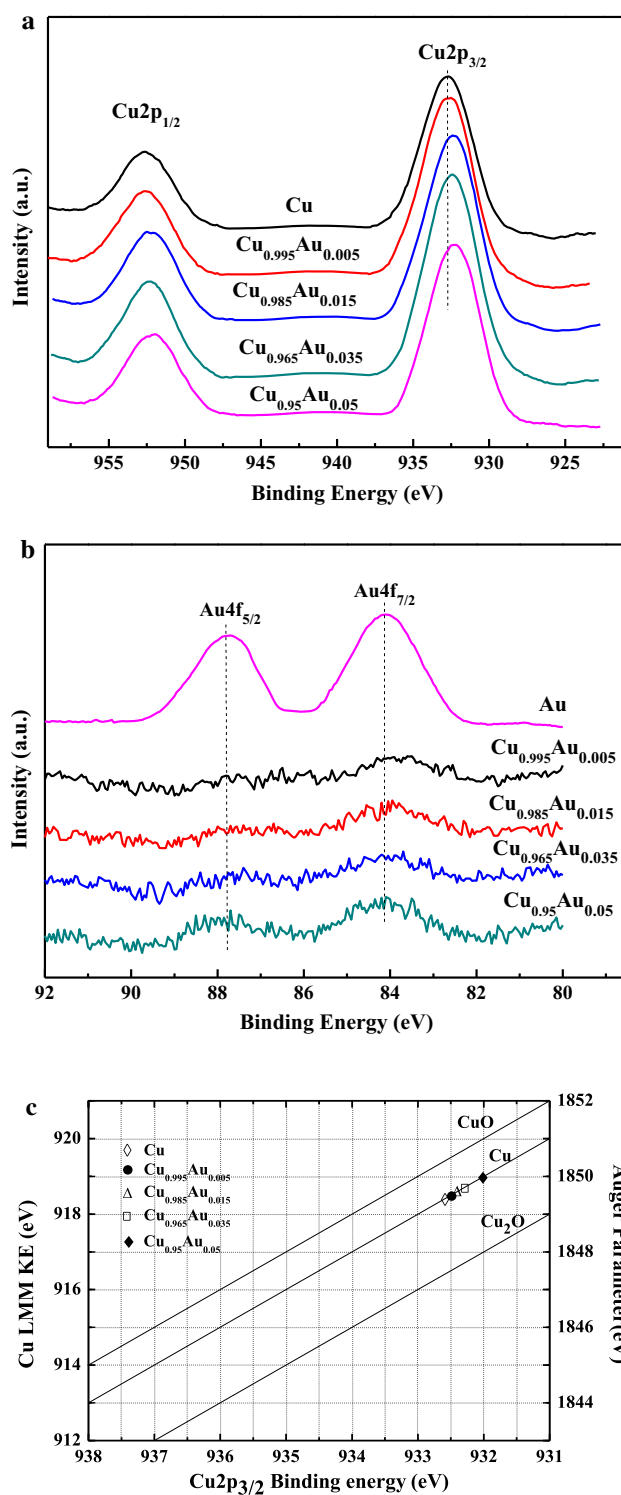


**Fig. 3** XPS spectra of Cu, Au,  $\text{Cu}_{0.95}\text{Au}_{0.05}$ ,  $\text{Cu}_{0.965}\text{Au}_{0.035}$ ,  $\text{Cu}_{0.985}\text{Au}_{0.015}$ , and  $\text{Cu}_{0.995}\text{Au}_{0.005}$  samples and Wagner plots of copper species

Cu nanoparticles were used as the catalysts, no conversion of 1,2-propanediol were found, revealing that monometallic Cu nanoparticles were not active for the oxidation of

**Table 2** The catalytic activities of the  $\text{Cu}_x\text{Au}_y$  nanoparticles for the catalytic oxidation of 1,2-propanediol

Catalysts	Conversions <sup>a</sup> (%)	Selectivities (%)			TOF <sup>b</sup> ( $\text{h}^{-1}$ )
		Formic acid	Lactic acid	Acetic acid	
Cu	0	0	0	0	0
$\text{Cu}_{0.995}\text{Au}_{0.005}$	34.0	10.6	70.3	19.1	1026
$\text{Cu}_{0.985}\text{Au}_{0.015}$	89.3	7.8	76.1	16.1	917
$\text{Cu}_{0.965}\text{Au}_{0.035}$	89.8	9.5	73.8	16.7	411
$\text{Cu}_{0.95}\text{Au}_{0.05}$	90.0	11.5	67.3	21.2	297
Au <sup>c</sup>	26.0	9.9	71.9	18.2	86
$\text{Cu}_{0.985}\text{Au}_{0.015}$ -controlled	68.9	10.1	69.2	20.8	707

<sup>a</sup> Reaction conditions: 1,2-propanediol concentration,  $0.28 \text{ mol L}^{-1}$ ; NaOH concentration,  $0.56 \text{ mol L}^{-1}$ ; volume of solution, 200 mL; catalyst, 0.06 g; reaction temperature,  $100 \text{ }^\circ\text{C}$ ; reaction time, 4 h; and stirring rate, 600 rpm

<sup>b</sup> TOF = The moles of converted 1,2-propanediol divided by moles of Au in  $\text{Cu}_x\text{Au}_y$  catalysts and reaction time, considering that pure Cu nanoparticles had no catalytic activity under our present reaction conditions

<sup>c</sup> The amount of Au nanoparticles used in the reaction was the same as that present in the  $\text{Cu}_{0.95}\text{Au}_{0.05}$  catalyst

1,2-propanediol under our present experimental conditions. When the monometallic Au nanoparticles were used as the catalysts, the conversion of 1,2-propanediol was 26.0 % and the selectivities of lactic acid, formic acid, and acetic acid were 71.9, 9.9, and 18.2 %, respectively. Au nanoparticles catalyzed the oxidation of 1,2-propanediol under the present experimental conditions.

When the Cu@Au nanoparticles were used as the catalysts, the 1,2-propanediol conversions increased from 34.0 to 90.0 % with increasing the Au ratio from 0.005 to 0.05. Maximum lactic acid selectivity of 76.1 % was obtained over the  $\text{Cu}_{0.985}\text{Au}_{0.015}$  nanoparticle catalyst. With further increasing Au ratio to 0.05, the selectivity of lactic acid decreased while the selectivities of formic and acetic acids increased. The Cu@Au nanoparticles with the mole ratios of Au to Cu of 0.015:0.985 and 0.035:0.965 exhibited high catalytic activities for the catalytic oxidation of 1,2-propanediol to lactic acid. The content of Au in the Cu@Au nanoparticles obviously affected the 1,2-propanediol conversion and product selectivity.

It was interesting to find that the TOF values ( $297\text{--}1026 \text{ h}^{-1}$ ) of bimetallic Cu@Au catalysts were 3.5–12 times higher than that of the monometallic Au nanoparticles ( $86 \text{ h}^{-1}$ ). According to XRD analysis, there existed an alloy trend between Cu and Au nanoparticles. It could be explained as that the coalesced Cu and Au nanoparticles synergistically catalyzed the selective oxidation of 1,2-propanediol to lactic acid.

When the bimetallic  $\text{Cu}_{0.985}\text{Au}_{0.015}$ -controlled catalyst prepared without organic modifier was used, the conversion of 1,2-propanediol and the selectivity of lactic acid were lower than those over the bimetallic  $\text{Cu}_{0.985}\text{Au}_{0.015}$  catalyst prepared by the use of organic modifier, respectively. The results indicated that the small-sized bimetallic

Cu@Au nanoparticles had higher catalytic activity for the oxidation of 1,2-propanediol to lactic acid than the large-sized ones.

Considering that the  $\text{Cu}_{0.985}\text{Au}_{0.015}$  catalyst gave high catalytic activity in the selective oxidation of 1,2-propanediol to lactic acid, it was selected as the model catalyst for investigating the effect of other reaction parameters on the catalytic oxidation of 1,2-propanediol.

### 3.5 Effect of Reaction Temperature

After reacting for 4 h under 1.0 MPa of  $\text{O}_2$  over the  $\text{Cu}_{0.985}\text{Au}_{0.015}$  catalyst, the conversions of 1,2-propanediol increased from 17.9 to 90.5 % with increasing the reaction temperatures from 60 to  $120 \text{ }^\circ\text{C}$  (Fig. 4). The selectivities of lactic acid increased from 64.0 to 76.1 % with increasing the reaction temperature from 60 to  $100 \text{ }^\circ\text{C}$ . With further increasing the reaction temperature to  $120 \text{ }^\circ\text{C}$ , the lactic acid selectivity slightly decreased to 72.6 %. The selectivities of formic and acetic acids were around 10 and 20 %, respectively. The results revealed that high reaction temperature favored the oxidation of 1,2-propanediol to lactic acid.

### 3.6 Effect of 1,2-Propanediol Concentration

After reacting at  $100 \text{ }^\circ\text{C}$  and 1.0 MPa of  $\text{O}_2$  for 4 h over the  $\text{Cu}_{0.985}\text{Au}_{0.015}$  catalyst, with increasing the 1,2-propanediol concentrations from 0.14 to 0.28, and  $0.42 \text{ mol L}^{-1}$ , the conversions of 1,2-propanediol decreased from 93.8 to 89.3 %, and 71.2 % (Fig. 5). Under the different 1,2-propanediol concentrations, the selectivities of lactic acid slightly decreased from 81.7 to 78.6 %, 79.7 to 76.1 %, and 74.5 to 69.7 %, respectively, with

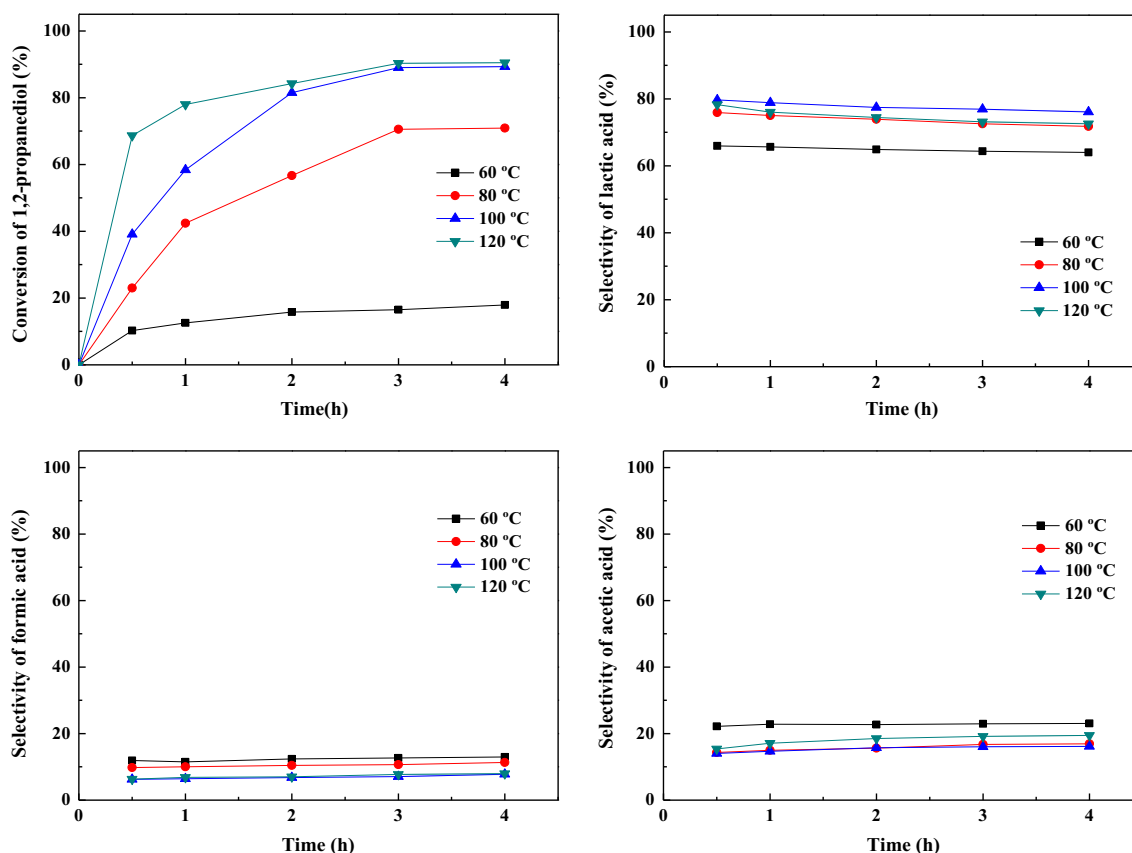


**Fig. 4** Effect of reaction temperature on the catalytic oxidation of 1,2-propanediol over  $\text{Cu}_{0.985}\text{Au}_{0.015}$  nanoparticles. Reaction conditions: 1,2-propanediol concentration,  $0.28 \text{ mol L}^{-1}$ ; NaOH

concentration,  $0.56 \text{ mol L}^{-1}$ ; volume of solution, 200 mL;  $\text{O}_2$  pressure, 1.0 MPa; catalyst loading, 0.06 g; stirring rate, 600 rpm

prolonging the reaction times from 0.5 to 4 h. The selectivities of formic acid and acetic acid were around 8 and 16 %, respectively. 1,2-Propanediol was efficiently oxidized to lactic acid at a low 1,2-propanediol concentration.

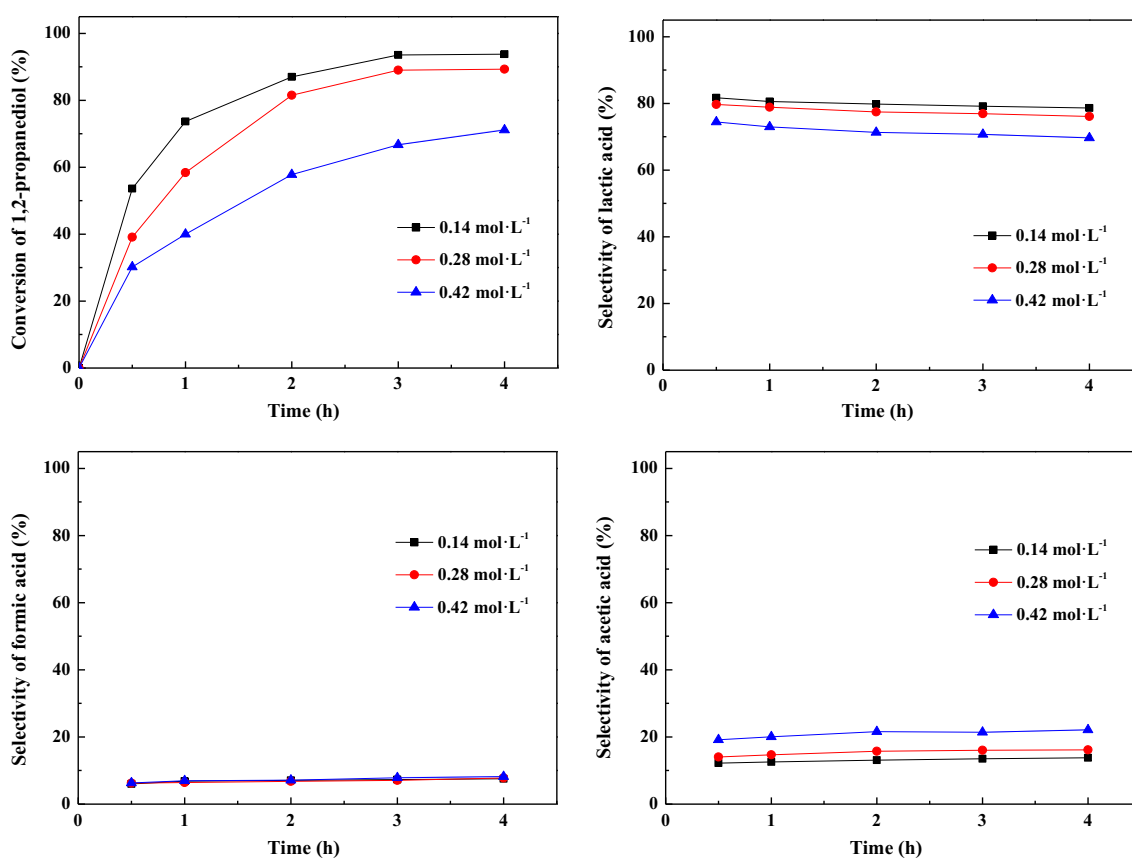
### 3.7 Effect of $\text{O}_2$ Pressure

Figure 6 shows the conversions of 1,2-propanediol and the selectivities of lactic acid, formic acid, and acetic acid over the  $\text{Cu}_{0.985}\text{Au}_{0.015}$  catalyst under different  $\text{O}_2$  pressures. After reacting at 100 °C for 4 h, with increasing the  $\text{O}_2$  pressures from 0.5 to 1.5 MPa, the conversions of 1,2-propanediol increased from 82.6 to 92.0 %. The selectivities of lactic acid decreased from 76.6 to 72.7 %. The selectivities of formic and acetic acids were around 8 to 16 %. The selectivities of formic and acetic acids slightly increased with the increase in the  $\text{O}_2$  pressures. The results demonstrated that high  $\text{O}_2$  pressure promoted the catalytic oxidation of 1,2-propanediol over the bimetallic  $\text{Cu}_{0.985}\text{Au}_{0.015}$  catalyst probably due to more active oxygen available. However, the presence of more active

oxygen also caused the formation of more formic and acetic acids.

### 3.8 Effect of NaOH Concentration

Figure 7 shows the conversions of 1,2-propanediol and the selectivities of lactic acid, formic acid, and acetic acid over the  $\text{Cu}_{0.985}\text{Au}_{0.015}$  catalyst under different NaOH concentrations. When the mole ratios of 1,2-propanediol to NaOH were 1:1, 1:2, and 1:3, the conversions of 1,2-propanediol were 60.0, 89.3, and 93.6 %, respectively, after reacting for 4 h. Under the different NaOH concentrations, the selectivities of lactic acid slightly decreased from 72.7 to 69.1 %, 79.7 to 76.1 %, and 81.8 to 78.5 % with prolonging the reaction time periods from 0.5 to 4 h. The selectivities of formic acid and acetic acid were around 7 and 15 %, respectively. The results revealed that high NaOH concentration was favorable to the selective oxidation of 1,2-propanediol to lactic acid. However, when the mole ratio of 1,2-propanediol to NaOH was equal to or less than 1:2, the selective oxidation of 1,2-propanediol to lactic



**Fig. 5** Effect of 1,2-propanediol concentration on the catalytic oxidation of 1,2-propanediol over  $\text{Cu}_{0.985}\text{Au}_{0.015}$  nanoparticles. Reaction conditions: NaOH concentration,  $0.56 \text{ mol L}^{-1}$ ; volume of

solution, 200 mL;  $\text{O}_2$  pressure, 1.0 MPa; reaction temperature,  $100 \text{ }^\circ\text{C}$ ; catalyst loading, 0.06 g; stirring rate, 600 rpm

acid was not obviously promoted by further increasing NaOH concentration.

### 3.9 Effect of Catalyst Loading

Figure 8 shows the conversions of 1,2-propanediol and the selectivities of lactic acid, formic acid, and acetic acid in the catalytic oxidation of 1,2-propanediol over the  $\text{Cu}_{0.985}\text{Au}_{0.015}$  catalyst with different catalyst loadings. After reacting at  $100 \text{ }^\circ\text{C}$  for 4 h with 1.0 MPa  $\text{O}_2$ , the 1,2-propanediol conversions increased from 73.7 to 89.3, and 94.2 % with increasing the catalyst loadings from 0.04 to 0.06, and 0.08 g. The results revealed that increasing catalyst loading obviously promoted the conversion of 1,2-propanediol due to more Au active sites available. When the catalyst loadings were 0.04, 0.06, and 0.08 g, with prolonging the reaction time from 0.5 to 4 h, the selectivities of lactic decreased from 80.7 to 77.6 %, 79.7 to 76.1 %, and 77.5 to 68.2 %. The selectivities of formic and acetic acids were around 7, 15 %; 8, 16 %; 10, 20 %, respectively. The results revealed that high catalyst loading not only favored the oxidation of 1,2-propanediol but also

caused the oxidation of intermediates to formic and acetic acids.

It is interesting to find that 1,2-propanediol was not completely converted under the present experimental conditions. The oxidation of 1,2-propanediol was probably inhibited by the interaction between the hydroxyl group of 1,2-propanediol and the carboxylate group of resultant lactate.

### 3.10 Reaction Kinetics

#### 3.10.1 Experimental Conditions for Kinetic Research

A power-function type reaction kinetic equation was used to evaluate the effect of 1,2-propanediol concentration,  $\text{O}_2$  pressure, and reaction temperature on the reaction rate over the  $\text{Cu}_{0.985}\text{Au}_{0.015}$  and  $\text{Cu}_{0.985}\text{Au}_{0.015}$ -controlled bimetallic nanoparticles. The effect of NaOH concentration on the reaction rate was ignored herein by setting a constant NaOH concentration in the experiments for evaluating the reaction kinetics. The side reactions for the formation of formic and acetic acids were ignored considering that the

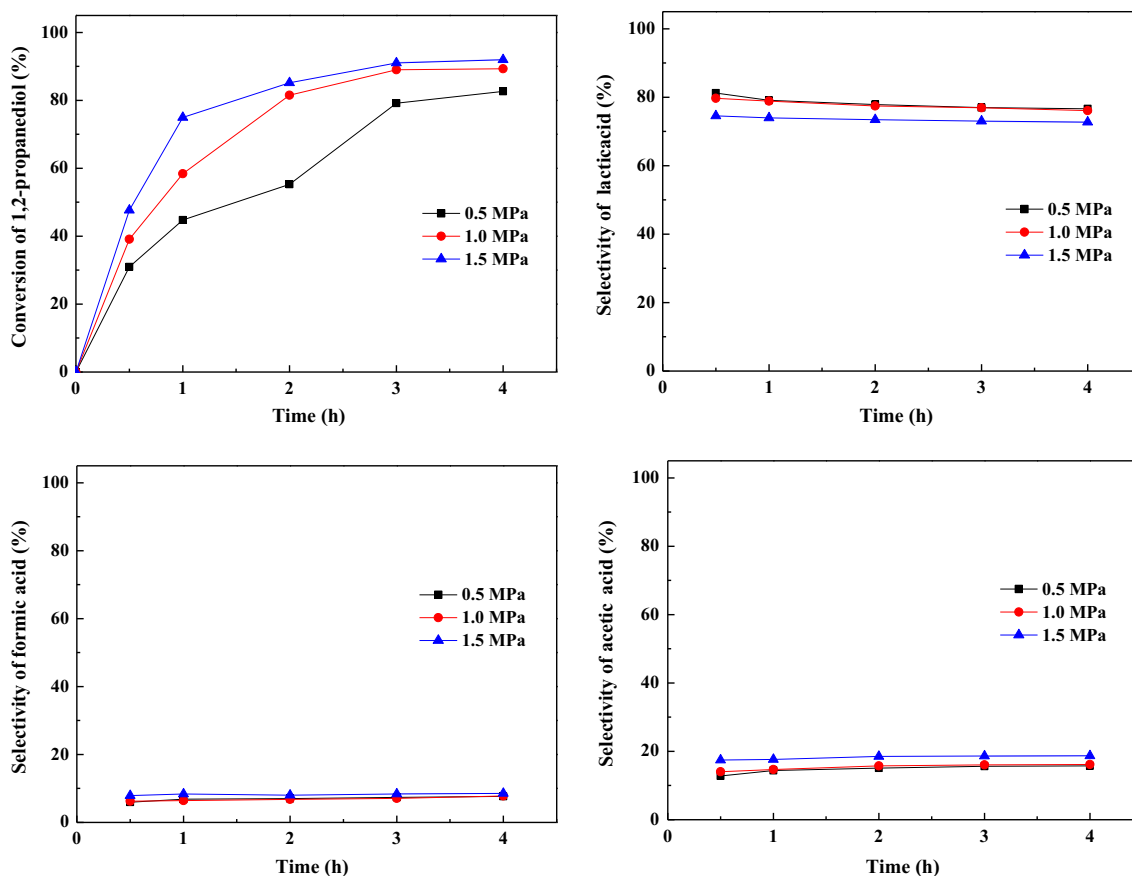


**Fig. 6** Effect of O<sub>2</sub> pressure on the catalytic oxidation of 1,2-propanediol over Cu<sub>0.985</sub>Au<sub>0.015</sub> nanoparticles. Reaction conditions: 1,2-propanediol concentration, 0.28 mol L<sup>-1</sup>; NaOH concentration,

0.56 mol L<sup>-1</sup>; volume of solution, 200 mL; reaction temperature, 100 °C; catalyst loading, 0.06 g; stirring rate, 600 rpm

initial reaction rates were used to fit the reaction kinetics and the amounts of formic and acetic acids were negligible at the initial reaction step.

In order to eliminate the mass diffusion, the Cu<sub>0.985</sub>Au<sub>0.015</sub> nanoparticles with the loadings of 0.04–0.08 g were used for the catalytic oxidation of 1,2-propanediol (0.28 mol L<sup>-1</sup>) at 100 °C for 0.5 h. Plotting catalyst loading vs 1,2-propanediol conversion gave a straight line (Fig. S1). According to Ref. [25], this result indicated that the catalytic oxidation reaction was controlled solely by chemical reaction rather than mass diffusion.

The power-function type reaction kinetic equation is expressed as Eq. (1).

$$r = -dn_0/(dt \cdot W_{cat}) = kC_0^a P_0^b \quad (1)$$

where  $k$  is the rate constant.  $a$  and  $b$  are the reaction orders with respect to the concentration of 1,2-propanediol and O<sub>2</sub> pressure.  $r$  is the initial reaction rate of 1,2-propanediol, mol h<sup>-1</sup> g<sup>-1</sup>.  $C_0$  is the initial concentration of 1,2-propanediol, mol L<sup>-1</sup>.  $P_0$  is the initial O<sub>2</sub> pressure, MPa.  $W_{cat}$  is the catalyst weight, g. The rate constant  $k$  follows the Arrhenius equation Eq. (2).

$$k = A \exp(-E_a/RT) \quad (2)$$

where  $A$  is the pre-exponential factor and  $E_a$  is the activation energy, kJ mol<sup>-1</sup>.  $R$  is the ideal gas constant, 8.314 × 10<sup>-3</sup> kJ mol<sup>-1</sup> K<sup>-1</sup>.  $T$  is the reaction temperature, K.

### 3.10.2 Determination of Reaction Orders

By taking the natural logarithm of both sides of the Eq. (1), a linear Eq. (3) is obtained as follows.

$$\ln r = \ln(-dn_0/(dt \cdot W_{cat})) = \ln k + a \ln C_0 + b \ln P_0 \quad (3)$$

To simulate the reaction orders of  $a$  and  $b$  according to Eq. (3), the initial reaction rates were calculated according to the data shown in Fig. S2. The initial reaction rates of 1,2-propanediol were calculated at the first 0.5 h.

By plotting  $\ln r$  vs  $\ln C_0$ , two straight lines over the Cu<sub>0.985</sub>Au<sub>0.015</sub> and Cu<sub>0.985</sub>Au<sub>0.015</sub>-controlled catalysts with the correlation coefficients of 0.9905 and 0.9965 were obtained, respectively (Fig. 9a). According to the slopes, over the Cu<sub>0.985</sub>Au<sub>0.015</sub> and Cu<sub>0.985</sub>Au<sub>0.015</sub>-controlled

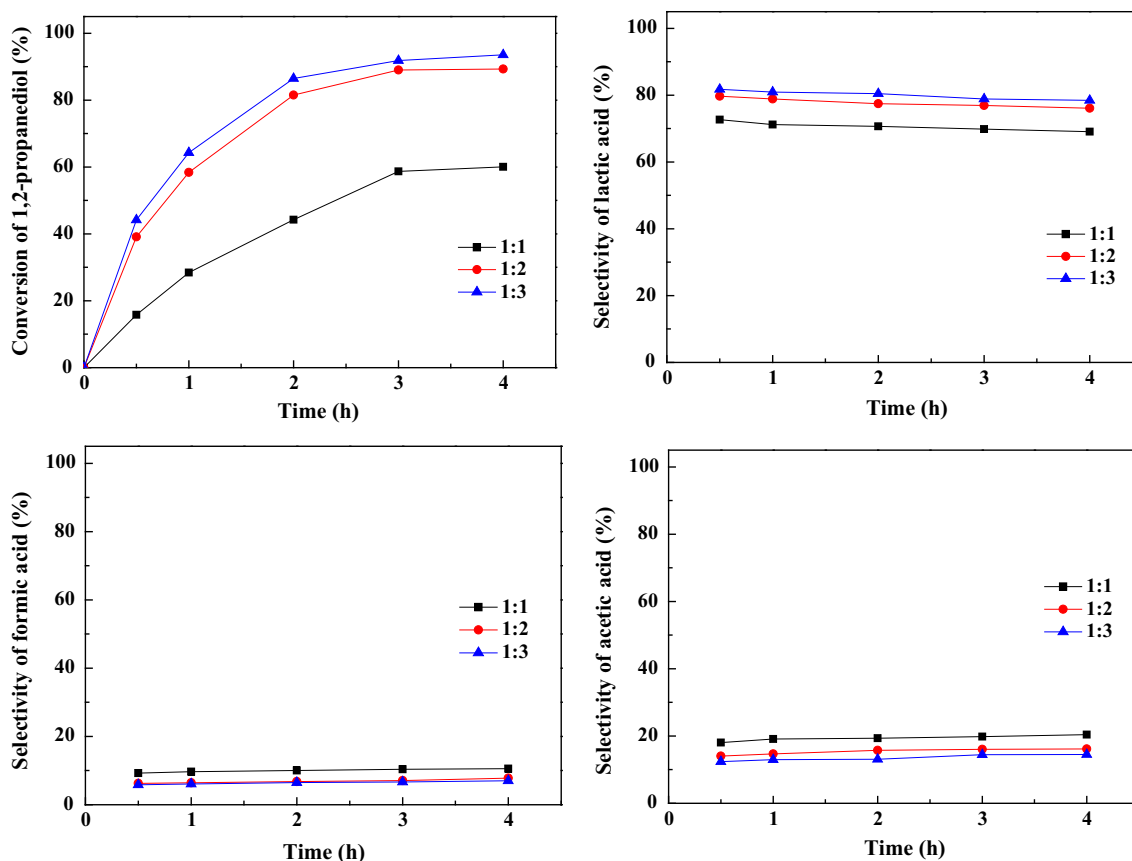


**Fig. 7** Effect of NaOH concentration on the catalytic oxidation of 1,2-propanediol over  $\text{Cu}_{0.985}\text{Au}_{0.015}$  nanoparticles. Reaction conditions: 1,2-propanediol concentration,  $0.28 \text{ mol L}^{-1}$ ; volume of

solution, 200 mL;  $\text{O}_2$  pressure, 1.0 MPa; reaction temperature,  $100 \text{ }^\circ\text{C}$ ; catalyst loading, 0.06 g; stirring rate, 600 rpm

catalysts, the reaction orders for 1,2-propanediol were 0.49 and 0.46, respectively.

By plotting  $\ln r$  vs  $\ln P_0$ , two straight lines over the  $\text{Cu}_{0.985}\text{Au}_{0.015}$  and  $\text{Cu}_{0.985}\text{Au}_{0.015}$ -controlled catalysts with the correlation coefficients of 0.9894 and 0.9957 were obtained, respectively (Fig. 9b). According to the corresponding slopes, the reaction orders for  $\text{O}_2$  were 0.39 and 0.45, respectively.

### 3.10.3 Activation Energy

Combined Eqs. (1) and (2), Eq. (4) is obtained as follows.

$$r = -dn_0/(dt \cdot W_{cat}) = A \exp(-Ea/RT) C_0^a P_0^b \quad (4)$$

By taking the natural logarithm of both sides, Eq. (4) can be rearranged as follows.

$$\ln r = \ln(-dn_0/(dt \cdot W_{cat})) = \ln(AC_0^a P_0^b) - (Ea/R)(1/T) \quad (5)$$

According to Eq. (5), two straight lines with the correlation coefficients of 0.9962 and 0.9908 over the

$\text{Cu}_{0.985}\text{Au}_{0.015}$  and  $\text{Cu}_{0.985}\text{Au}_{0.015}$ -controlled catalysts were obtained while plotting  $\ln r$  vs  $1/T$  (Fig. 9c). The data of the reaction rates,  $r$ , at different reaction temperatures were calculated by using the data shown in Fig. S3. The reaction activation energies ( $E_a$ ) and pre-exponential factors ( $A$ ) were calculated according to the slopes and intercepts of the straight lines. Over the  $\text{Cu}_{0.985}\text{Au}_{0.015}$  and  $\text{Cu}_{0.985}\text{Au}_{0.015}$ -controlled catalysts, the reaction kinetics were listed as follows.

$$r = -dn_0/(dt \cdot W_{cat}) = 80390 \exp(-34.1/RT) C_0^{0.49} P_0^{0.39} \text{ mol h}^{-1} \text{ g}^{-1} \quad (6)$$

$$r = -dn_0/(dt \cdot W_{cat}) = 14451759 \exp(-52.3/RT) C_0^{0.46} P_0^{0.45} \text{ mol h}^{-1} \text{ g}^{-1} \quad (7)$$

The reaction activation energy ( $34.1 \text{ kJ mol}^{-1}$ ) over the  $\text{Cu}_{0.985}\text{Au}_{0.015}$  catalyst was lower than that ( $52.3 \text{ kJ mol}^{-1}$ ) over the  $\text{Cu}_{0.985}\text{Au}_{0.015}$ -controlled catalyst. The small-sized bimetallic Cu@Au nanocatalyst exhibited higher catalytic activity for 1,2-propanediol oxidation than the large-sized one. Furthermore, the

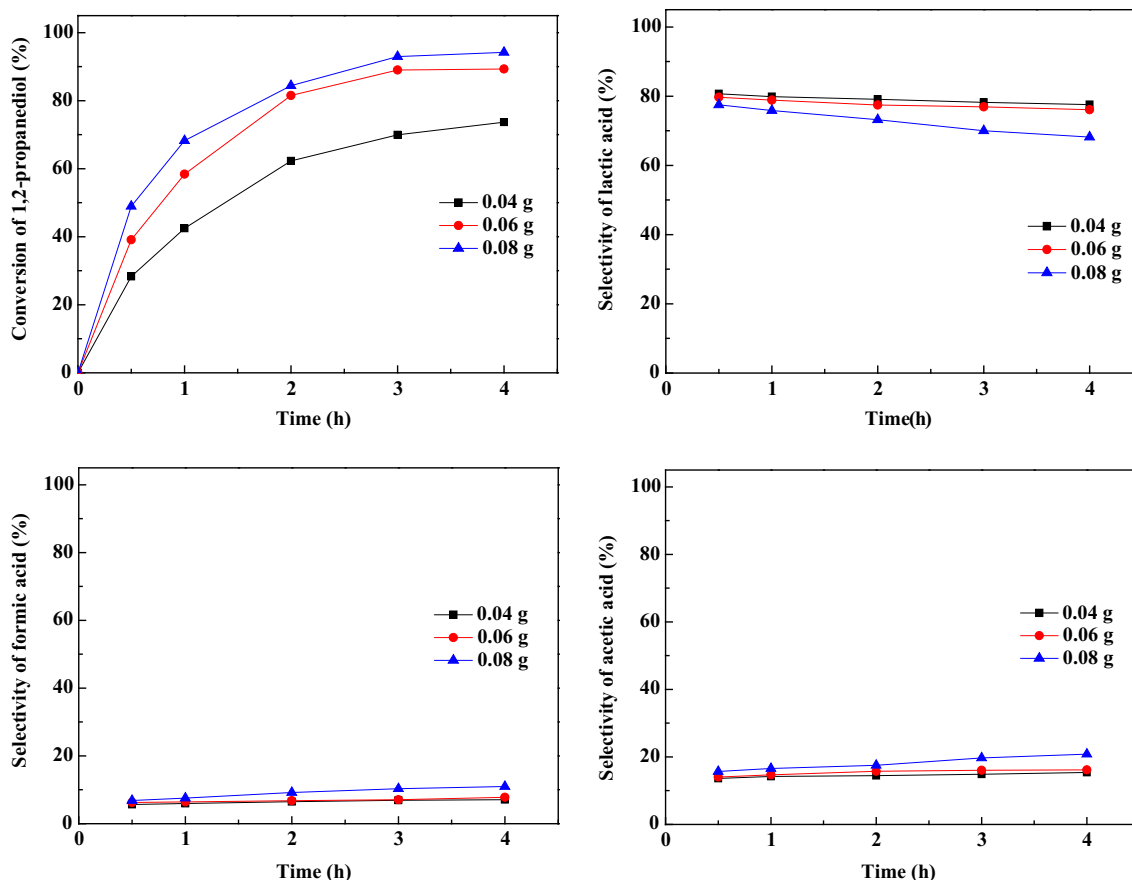


**Fig. 8** Effect of catalyst loading on the catalytic oxidation of 1,2-propanediol over  $\text{Cu}_{0.985}\text{Au}_{0.015}$  nanoparticles. Reaction conditions: 1,2-propanediol concentration,  $0.28 \text{ mol L}^{-1}$ ; NaOH concentration,

$0.56 \text{ mol L}^{-1}$ ; volume of solution, 200 mL;  $\text{O}_2$  pressure, 1.0 MPa; reaction temperature,  $100 \text{ }^\circ\text{C}$ ; stirring rate, 600 rpm

difference in the reaction orders for 1,2-propanediol and  $\text{O}_2$  indicated that the particle sizes of bimetallic Cu@Au nanoparticles significantly affected their catalytic activities.

### 3.11 Catalyst Recycling Performance

The recycling performances of the  $\text{Cu}_{0.985}\text{Au}_{0.015}$  bimetallic nanoparticles for the catalytic oxidation of 1,2-propanediol to lactic acid are shown in Fig. 10. After reacting at  $100 \text{ }^\circ\text{C}$  for 4 h, the reaction mixture was cooled down to room temperature. The used catalyst was centrifugated and washed with anhydrous ethanol. Then, the recovered catalyst was used directly in the oxidation reaction. No obvious change in the catalytic activity and product selectivity was observed after running for five times. The results revealed that the  $\text{Cu}_{0.985}\text{Au}_{0.015}$  bimetallic nanoparticle catalyst had good recycling performance for the selective oxidation of 1,2-propanediol to lactic acid.

## 4 Conclusions

The as-prepared Cu@Au core/shell nanoparticles were composed of Cu and Au nanoparticles with the average diameters of ca. 60 and 5 nm, respectively. The Au nanoparticles were well anchored on the surfaces of Cu nanoparticles to form the core/shell structure. The use of Tween as the organic modifier favored the formation of small-sized Cu and Au nanoparticles in the Cu@Au core/shell nanoparticles.

The Cu@Au nanoparticles with the mole ratios of Au to Cu of 0.015:0.985 and 0.035:0.965 exhibited high catalytic activities for the catalytic oxidation of 1,2-propanediol to lactic acid. When the catalytic oxidation of 1,2-propanediol was carried out over the  $\text{Cu}_{0.985}\text{Au}_{0.015}$  nanoparticles under 1.0 MPa of  $\text{O}_2$  at  $100 \text{ }^\circ\text{C}$  for 4 h in an alkaline solution, the lactic acid selectivity was 76.1 % at the 1,2-propanediol conversion of 89.3 %. The  $\text{Cu}_{0.985}\text{Au}_{0.015}$  nanoparticle catalyst had good recycling performance for the catalytic oxidation of 1,2-propanediol to lactic acid. Over the

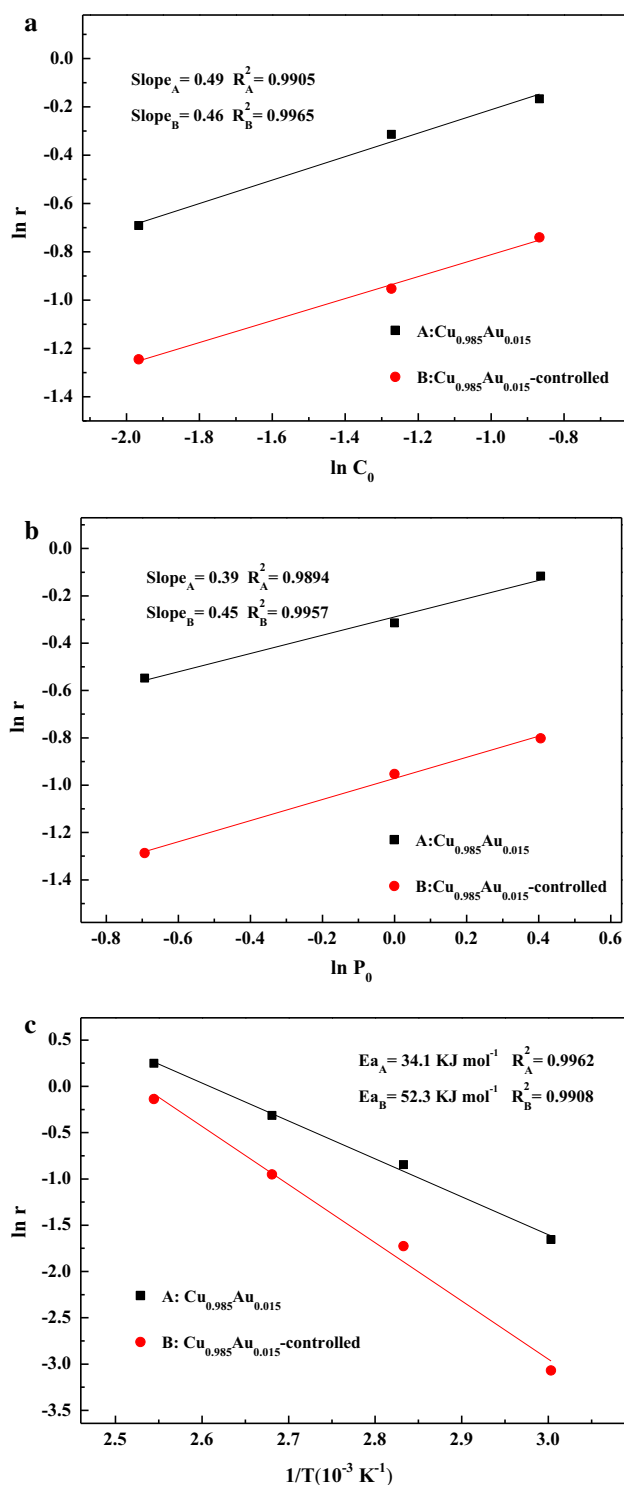


**Fig. 9** Estimation of (a, b) the reaction orders and (c) the reaction activation energies for the power-function type reaction kinetics over Cu<sub>0.985</sub>Au<sub>0.015</sub> and Cu<sub>0.985</sub>Au<sub>0.015</sub>-controlled catalysts

Cu<sub>0.985</sub>Au<sub>0.015</sub> catalyst, a power-function type reaction kinetic model well fitted the experimental data,  $r = -dn_0/(dt \cdot W_{cat}) = kC_0^{0.49}P_0^{0.39}$ , and the reaction activation energy was 34.1 kJ mol<sup>-1</sup>.

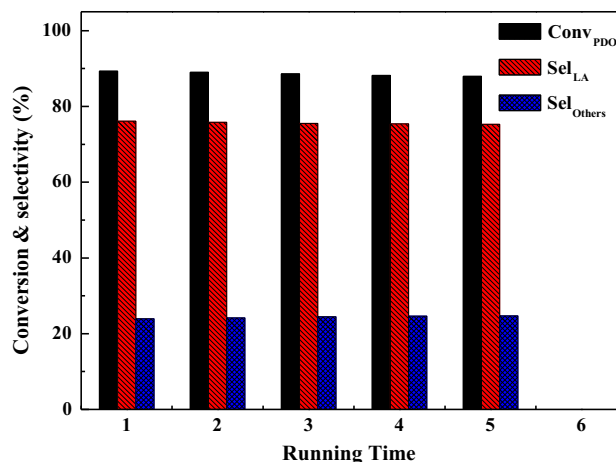


**Fig. 10** Recycling performance of Cu<sub>0.985</sub>Au<sub>0.015</sub> catalyst for the catalytic oxidation of 1,2-propanediol. Reaction conditions: 1,2-propanediol concentration, 0.28 mol L<sup>-1</sup>; NaOH concentration, 0.56 mol L<sup>-1</sup>; volume of solution, 200 mL; O<sub>2</sub> pressure, 1.0 MPa; reaction temperature, 100 °C; and stirring rate, 600 rpm; reaction time period, 4 h

**Acknowledgments** The work was financially supported by the funds from National Natural Science Foundation of China (21506078 and 21506082) and Science and Technology Department of Jiangsu Province (BY2014123-10).

## References

- Purushothaman RKP, van Haveren J, van Es DS, Melián-Cabrera I, Meeldijk JD, Heeres HJ (2014) Appl Catal B 147:92
- Marques FL, Oliveira AC, Filho JM, Rodríguez-Castellón E, Cavalcante CL Jr, Vieira RS (2015) Fuel Process Technol 138:228
- Cho HJ, Chang C-C, Fan W (2014) Green Chem 16:3428
- Maki-Arvela P, Simakova IL, Salmi T, Murzin DY (2014) Chem Rev 114:1909
- Yang GY, Ke YH, Ren HF, Liu CL, Yang RZ, Dong WS (2016) Chem Eng J 283:759
- Dusselier M, Van Wouwe P, Dewaele A, Makshina E, Sels BF (2013) Energ Environ Sci 6:1415
- Sikder J, Chakraborty S, Pala P, Drilic E, Bhattacharjee C (2012) Biochem Eng J 69:130
- Katryniok B, Paul S, Dumeignil F (2010) Green Chem 12:1910
- Fan YX, Zhou CH, Zhu XH (2009) Catal Rev 51:293
- Corma A, Iborra S, Velty A (2007) Chem Rev 107:2411
- Feng YH, Yin HB, Gao DZ, Wang AL, Shen LQ, Meng MJ (2014) J Catal 316:67
- Datta R, Henry M (2006) J Chem Technol Biotechnol 81:1119
- Prati L, Rossi M (1998) J Catal 176:552
- Narayanan N, Roychoudhury PK, Srivastava A (2004) Microb Biotechnol 7:167
- Bhanage BM, Fujita S, Ikushima Y, Arai M (2003) Green Chem 5:429
- <http://www.docin.com/p-445508830.html>
- <http://mcgroup.co.uk/news/20140418/propylene-glycol-market-rea-chsupplydemand-balance-2015.html>
- Tsujino T, Ohigashi T, Sugiyama S, Kawashiro K, Hayashi H (1992) J Mol Catal 71:25

19. Pinxt HHCM, Kuster BFM, Marin GB (2000) *Appl Catal A* 191:45
20. Ma H, Nie X, Cai JY, Chen C, Gao J, Miao H, Xu J (2010) *Sci China Chem* 53:1497
21. Dimitratos N, Lopez-Sanchez JA, Meenakshisundaram S, Anthonykutti JM, Brett G, Carley AF, Taylor SH, Knight DW, Hutchings GJ (2009) *Green Chem* 11:1209
22. Feng YH, Yin HB, Wang AL, Gao DZ, Zhu XY, Shen LQ, Meng MJ (2014) *Appl Catal A* 482:49
23. Feng YH, Yin HB, Wang AL, Xue WP (2015) *J Catal* 326:26
24. Carrettin S, McMorn P, Johnston P, Griffin K, Hutchings GJ (2002) *Chem Commun* 7:696
25. Huang XM, Wang XG, Wang XS, Wang XX, Tan MW, Ding WZ, Lu XG (2013) *J Catal* 301:217
26. Dai WL, Sun Q, Deng JF, Wu D, Sun YH (2001) *Appl Surf Sci* 177:172